Finite Differences

Numerical Analysis of Maxwell's Equations

Finn Joel Bjervig*and John Danielsson†

1TD050 - Advanced Numerical Methods,
Department of Information Technology,
Uppsala university, Sweden

August 31, 2022

*Electronic address: jobj8920@student.uu.se
†Electronic address: joda2016@student.uu.se

1 Assignment 1

1.1 Model Description and The Energy Method

The PDE describes Maxwell's equations in 1D.

$$Cu_t = Au_x \qquad x \in [x_l, x_r], t \leq 0 \tag{1}$$
$$L_l u = g_l(t) \qquad x = x_l \tag{2}$$
$$L_r u = g_r(t) \qquad x = x_r \tag{3}$$

where

$$C = \begin{pmatrix} \epsilon_0 & 0 \\ 0 & \mu_0 \end{pmatrix} \qquad A = \begin{pmatrix} 0 & 1 \\ 1 & 0 \end{pmatrix} \qquad u = \begin{bmatrix} E \\ H \end{bmatrix} \tag{4}$$

E and H are the electric and magnetic field components and μ_0 is the vacuum permeability and ϵ_0 the vacuum permittivity. $c = 1/\sqrt{\epsilon_0 \mu_0}$ is the speed of light in a vacuum and $Z_0 = \sqrt{\epsilon_0/\mu_0}$ is the vacuum impedance.

Normalizing the PDE will make make the matrix C into the Identity matrix, consequently changing the wave propagation speed from $\pm c$ to ± 1. We denote this new coefficient matrix as

$$\tilde{C} = \begin{pmatrix} 1 & 0 \\ 0 & 1 \end{pmatrix}$$

The first task is to specify two types of boundary conditions; Dirichlet and Characteristic, and determine the *how many* are needed.

First step in the energy method is to multiply the PDE with u^* on both sides and integrate by parts.

$$(u, u_t)_C = (u, Au_x) = u^* Au|_{x=x_l}^{x=x_r} - (u_x, Au) \tag{5}$$

Thereafter, consider the conjugate transpose of 5

$$(u, u_t)_C^* = (u, Au_x)^* = (u_x, A^* u) \tag{6}$$

and add this to 5. This is referred to as the energy method.

$$(u_t, u)_C + (u, u_t)_C = u^* Au|_{x=x_l}^{x=x_r} + (u_x, (A - A^*)u) \tag{7}$$

Since $A = A^*$, the last term is eliminated. We can rewrite the LHS using the differentiation product rule in reverse and RHS by evaluating the matrix vector multiplication. This leaves us with the energy estimate

$$dt||u||_C^2 = 2u_1u_2|_{x=x_r} - 2u_1u_2|_{x=x_l} \leq 0 \tag{8}$$

For the energy estimate to be bound to at or below zero we can see that we will need one boundary condition at each boundary.

One set of Dirichlet boundary conditions may look like

$$\begin{aligned} L_l u_1 &= u_1|_{x=x_l} = g_l(t) \\ L_r u_1 &= u_1|_{x=x_r} = g_r(t) \end{aligned} \tag{10}$$

Characteristic boundary conditions requires us to investigate the characteristic variables. We start by transforming the PDE using these characteristic variables

$$\tilde{u}_t = C^{-1}A\tilde{u}_x = B\tilde{u}_x \qquad x \in [x_l, x_r], t \leq 0 \tag{11}$$

$$L_l\tilde{u} = g_l(t) \qquad x = x_l \tag{12}$$

$$L_r\tilde{u} = g_r(t) \qquad x = x_r \tag{13}$$

$$\tag{14}$$

It is necessary that B is hermitian, and if not, we need to diagonalize it. In this case B is indeed Hermitian since

$$B^* = B = \tilde{C}^{-1}A = \begin{pmatrix} 0 & 1 \\ 1 & 0 \end{pmatrix} \tag{15}$$

U diagonalizes the PDE's matrix B and its columns are the eigenvectors of B while Λ has the eigenvalues of B on its diagonal

$$\tilde{u} = U^{-1}u \qquad U^tBU = \Lambda \tag{16}$$

$$U = \frac{1}{\sqrt{2}}\begin{pmatrix} -1 & 1 \\ 1 & 1 \end{pmatrix} \qquad \Lambda = \begin{pmatrix} -1 & 0 \\ 0 & 1 \end{pmatrix} \tag{17}$$

The characteristic variables are thus

$$\tilde{u} = U^{-1}u = \frac{1}{\sqrt{2}}\begin{bmatrix} -u_1 + u_2 \\ u_1 + u_2 \end{bmatrix} \tag{18}$$

From which we deduce that the characteristic boundary conditions are

$$L_l u = -u_1 + u_2 = g_l(t) \qquad x = x_l \tag{19}$$
$$L_r u = u_1 + u_2 = g_r(t) \qquad x = x_r \tag{20}$$

the scalar $1/\sqrt{2}$ is included in g.

1.2 SBP-SAT discretization

The second task is to approximate the PDE using the SBT-SAT method for the two types of initial conditions derived in task 1 (Diriclet and Characteristic). Thereafter we derive the energy estimate to see what the conditions are for stability.The SBT-SAT method is a semi-discretization because time is left continuous throughout the analysis. It can be discretized using RK4 or similar time schemes.

Dirichlet Boundary conditions

The semi-discrete version of the Dirichlet boundary conditions 10 are

$$L_l v_1^{(1)} = v_1^{(1)}|_{x=x_l} = g_l(t)$$
$$L_r v_m^{(1)} = v_m^{(1)}|_{x=x_r} = g_r(t)$$

SBT-SAT sets up the following semi-discrete problem

$$(B \otimes D_1)v + \tau_l \otimes H^{-1}e_1(v_1^{(1)} - g_l(t)) - \tau_r \otimes H^{-1}e_m(v_m^{(1)} - g_r(t)) \tag{21}$$

where the penalty vector $\tau_{l,r} = \left[\tau_{l,r}^{(1)}; \tau_{l,r}^{(2)}\right]^T$ for the respective boundaries determines the stability of the scheme. The conditions for stability are

$$\begin{bmatrix} \tau_l^{(1)} \leq 1 \\ \tau_l^{(2)} = 1 \end{bmatrix} \qquad\qquad \begin{bmatrix} \tau_r^{(1)} \leq 1 \\ \tau_r^{(2)} = -1 \end{bmatrix} \tag{22}$$

such that the semi-discrete energy estimate for stability is fulfilled

$$\frac{d}{dt}||u||_H^2 = 2\tau_l^{(1)}(v_1^{(1)})^2 + 2\tau_r^{(1)}(v_m^{(1)})^2 \leq 0 \tag{23}$$

Characteristic Boundary conditions

We can split up the B matrix into two matrices such that we group the eigenvalues based on its sign. B_- has negative eigenvalues and B_+ has only positive.

This is achieved using Warming flux splitting

$$B_\pm = U^T(\Lambda \pm |\Lambda|)U \tag{24}$$

$$B_- = \frac{1}{2}\begin{pmatrix} -1 & 1 \\ 1 & -1 \end{pmatrix} \qquad\qquad B_+ = \frac{1}{2}\begin{pmatrix} 1 & 1 \\ 1 & 1 \end{pmatrix}$$

impose BC on the characteristic variables as in 19 which is equivalent to

$$B_- u = B_- g_l(t) \qquad x = x_l \tag{25}$$
$$B_+ u = B_+ g_r(t) \qquad x = x_r \tag{26}$$

The SBT-SAT approximation reads as

$$v_t = (A \otimes D_1)v - B_+ \otimes H^{-1} e_m(v_m - g_r(t)) + B_- \otimes H^{-1} e_1(v_1 - g_l(t)) \tag{27}$$

for which the energy estimate becomes

$$\frac{d}{dt}||v||_H^2 = BT_r + BT_l \tag{28}$$

where the left and right boundary terms $BT_{r,l}$ are

$$BT_r = \quad +v_m^T A_- v_m \quad +g_r(t)^T A_+ g_r(t) \quad -(v_m - g_r)^T A_+ (v_m - g_r) \tag{29}$$
$$BT_l = \quad -v_1^T A_+ v_1 \quad +g_l(t)^T A_- g_l(t) \quad -(v_1 - g_l)^T A_- (v_1 - g_l) \tag{30}$$

The semi-discrete solution can be bounded using the boundary data, and is thus stable.

1.3 SBP-Projection discretization

The third task is to consider a projection method for imposing BC to guarantee stability. Below is the same PDE as before. (matrix A is equal to B, for the sake of not mixing notations up)

$$\begin{aligned} v_t &= Av_x \qquad t \leq 0 \\ Lv &= g(t) \end{aligned}$$

We start with the Dirichlet BC operator 10 and discretize it. Here are some vector definitions

$$L_d = \begin{bmatrix} e^1 \otimes e_1^T \\ e^1 \otimes e_m^T \end{bmatrix} \qquad L_c = \begin{bmatrix} e^2 \otimes e_1^T - e^1 \otimes e_1^T \\ e^2 \otimes e_m^T + e^1 \otimes e_m^T \end{bmatrix} \tag{31}$$

$$e^1 = (1,0) \qquad e^2 = (0,1) \tag{32}$$

$$v = \left[v_1^{(1)}, v_1^{(2)}, \ldots, v_1^{(m)}, v_2^{(1)}, v_2^{(2)}, \ldots, v_2^{(m)}\right]^T \qquad g(t) = \begin{bmatrix} g_l(t) \\ g_r(t) \end{bmatrix} \tag{33}$$

The SBT-Projection matrix is defined as

$$P = I - H^{-1}L^T(LH^{-1}L^T)^{-1}L \tag{34}$$

, which is stable if the energy estimate is satisfied

$$\frac{d}{dt}||v||_H^2 = -(Pv)_1^T A(Pv)_1 + (Pv)_m^T A(Pv)_m = 0 \tag{35}$$

The Matrix H is later defined and is a differentiation quadrature.

1.4 Implementation

The SBP-SAT and SBP-Projection implementations both lead to systems of equation such that $\frac{d}{dt}v = Dv$, with the discretization matrix D being

$$D = A \otimes D_1 + SAT_l + SAT_r \qquad \text{for SBP-SAT} \tag{36}$$

$$D = P(A \otimes D_1)P \qquad \text{for SBP-Projection} \tag{37}$$

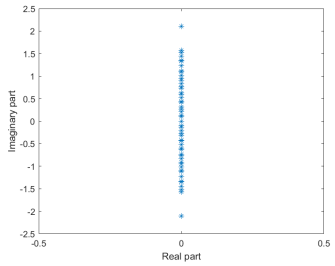

(a) SBP-SAT with Dirichlet B.Cs

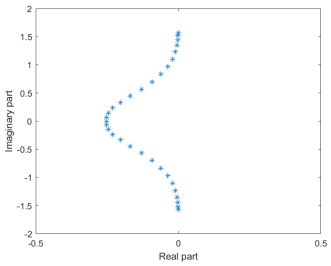

(b) SBP-SAT with Characteristic B.Cs

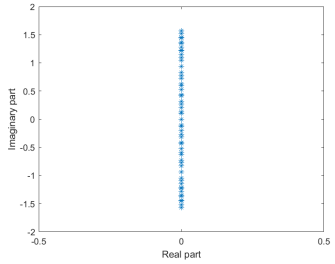

(c) SBP-Projection with Dirichlet B.Cs

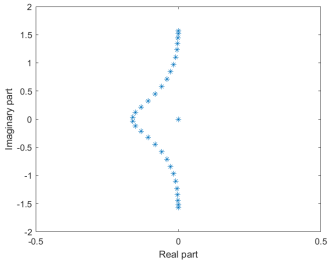

(d) SBP-Projection with characteristic B.Cs

Figure 1: Real and imaginary parts of eigenvalues for the different schemes and B.Cs

These systems are stable if no eigenvalues of the matrices have positive real parts.

The eigenvalues are computed using the Matlab eigs() function and shown in figure 1. The eigenvalues for all different schemes and boundary conditions have a real part less or equal to zero, showing that the methods are stable. For the chosen Dirichlet boundary conditions all eigenvalues are completely imaginary, while for the characteristic boundary conditions many have a negative real part.

The parameters for the SAT and projection discretizations are chosen from the result of the energy estimate with Dirichlet and characteristic boundary conditions respectively (SAT, Dirichlet: 23, SAT, characteristic :28, and projection: 35) such that the implementations in fact are stable.

The CFL number is denoted α and describes the fraction $\alpha = \frac{\Delta x}{\Delta t}$ that leads to a stable solution. The CFL number and maximum time-step will depend on the time integration scheme, here RK4, as well as the discretization matrices of the systems given in 36 and 37. RK4 is stable if all eigenvalues of the matrix D are within its region of stability so that

$$k\left|\lambda_{max}\right| \leq 2.82 \Rightarrow k \leq \frac{2.82}{\left|\lambda_{max}\right|} \Rightarrow \alpha \approx \frac{2.82}{h\left|\lambda_{max}\right|} \tag{38}$$

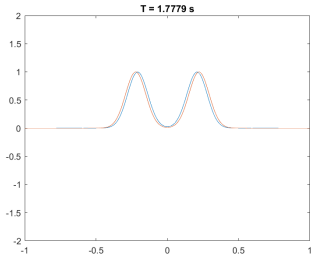

(a) Using $\alpha = 1.45$ for determining timestep

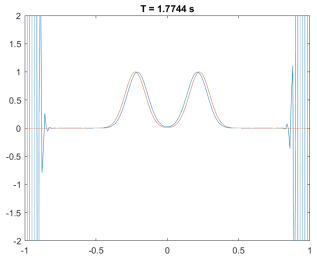

(b) Using $\alpha = 1.6$ for determining timestep

Figure 2: Comparison for solving SBP-SAT using different $k = \alpha h$

For the matrix from SBP-SAT with Dirichlet B.Cs and $[\tau_l, \tau_r] = \left(\begin{smallmatrix} 0 & 1 \\ 0 & -1 \end{smallmatrix}\right)$ we have $\alpha \approx 1.45$ while for the matrix from SBP-Projection we have $\alpha \approx 2.05$.

When using characteristic B.Cs both SBP-SAT and SBP-Projection have an α of around 2.05, which seems reasonable as the matrices of all these systems have similar max eigenvalues, as can be seen in figure 1.

This appears to correspond well with numerical results as using time-steps larger than the given α gives unstable solutions while smaller seem to remain stable over time as seen in figure 2.

To compute the convergence rate of the implementations we can compare them to an analytical solution given by

$$u^{(1)}(x,t) = \theta^{(1)}(x, L-t) - \theta^{(2)}(x, L-t), \quad u^{(2)}(x,t) = \theta^{(1)}(x, L-t) + \theta^{(12)}(x, L-t) \tag{39}$$

with $\theta^{(1,2)}$ being given by

$$\begin{cases} \theta^{(1)}(x,t) = \exp(-(\frac{x-t}{r_*})^2) \\ \theta^{(2)}(x,t) = -\exp(-(\frac{x+t}{r_*})^2) \end{cases} \tag{40}$$

and using the following initial conditions for the solution

$$u^{(1)}(0,t) = \theta^{(2)}(x,0) - \theta^{(1)}(x,0), \quad u^{(2)}(x,t) = \theta^{(1)}(x,0) + \theta^{(2)}(x,0) \tag{41}$$

We can calculate the convergence rate for the solution using

$$\log_{10}\left(\frac{\left\|u - v^{(m_1)}\right\|}{\left\|u - v^{(m_2)}\right\|}\right) \Big/ \log_{10}\left(\frac{m_1}{m_2}\right)^{\frac{1}{d}} \tag{42}$$

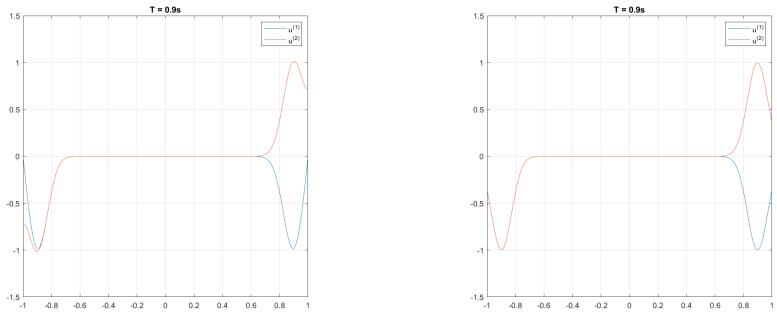

(a) Solution at t = 0.9s using Dirichlet B.Cs (b) Solution at t = 0.9s using characteristic B.Cs

Figure 3: Numerical SBP-SAT solution using different B.Cs using h = 201

m	$\log_{10}(\mathrm{L}^2)_{SAT}$	q_{SAT}	$\log_{10}(\mathrm{L}^2)_{Proj}$	q_{Proj}
51	-0.7373	-	-0.7552	-
101	-1.6711	3.1469	-1.6569	3.0385
201	-2.8996	4.1102	-2.7222	3.5644
401	-3.7054	2.6867	-3.5616	2.7983

Table 1: Convergence rate q for SBP-SAT and SBP-Projection

with the norms for vectors being $\|v\|_h = \sqrt{h\sum_{i=1}^{m}|v_i|^2}$ and d describing the dimension, here 1. This is done for several values of h in table 1.

The numerical solution here appears to have a convergence rate around 3 for both SAT and Projection methods.

The solution at t=0.9s is plotted using both Dirichlet and characteristic boundary conditions in figure 3. We can see that for the Dirichlet condition $u^{(1)}$ is bound to zero at the left and right boundary while $u^{(2)}$ is free. For characteristic boundary conditions the vectors $u^{(1)}$ and $u^{(2)}$ are bound so that $u^{(2)} - u^{(1)} = 0$ at the left side and $u^{(1)} + u^{(1)} = 0$ at the right side as described in equation 19 & 20. These boundary conditions leads the solution to disappear over the boundary.

2 Assignment 2

2.1 Interface Conditions

In this assignment we explore the two equations

$$C^{(l)}u_t = Au_x \qquad u \in [x_l, x_I] \tag{43}$$
$$C^{(r)}v_t = Av_x \qquad v \in [x_I, x_r] \tag{44}$$

with $C^{(l,r)}$ being given by

$$C^{l,r} = \begin{pmatrix} \epsilon^{(l,r)} & 0 \\ 0 & \mu \end{pmatrix} \tag{45}$$

At the interface waves with different ϵ split into reflection and transmission waves. For a 1D wave going from left to right, after it has split at the interface the magnitude of the reflection (R) and transmission (T) are given by

$$T = \frac{2\eta^{(l)}}{\eta^{(l)} + \eta^{(r)}}, \qquad R = \frac{\eta^{(l)} - \eta^{(r)}}{\eta^{(l)} + \eta^{(r)}} \tag{46}$$

with $\eta^{(l,r)}$ being the refractive indices given by $\sqrt{\epsilon^{(l,r)}}$.

To find the necessary boundary and interface conditions to the equations, we can calculate the combined energy estimate

$$\begin{aligned} \frac{\mathrm{d}}{\mathrm{dt}} \left(\|u\|^2_{C_1} + \|v\|^2_{C_w} \right) &= (u, C_1 u_t) + (u_t, C_1 u) + (v, C_2 v_t) + (v_t, C_2 v) \\ &= u^* A u|^{x_I} - u^* A u|^{x_l} + v^* A v|^{x_r} - v^* A v|^{x_I} \\ &= v_{(1)} v_{(2)}|^{x_r} + (u_{(1)} u_{(2)} - v_{(1)} v_{(2)})|^{x_I} - u_{(1)} u_{(2)}|^{x_l} \leq 0 \end{aligned} \tag{47}$$

At the outer boundaries $x_{l,r}$ the boundary conditions can be chosen in the same way as described in the first assignment. For the interface conditions we need that $u = v,$ on $\mathrm{x} = \mathrm{x}_I$ for the interface term to disappear in the energy estimate.

2.2 SBP-SAT approximation

With D_1 being a first derivative SBP operator the SBP-SAT approximation can be written as

$$C_1 u_t = (A \otimes D_1)u + \sigma_l A^+ \otimes H^{-1} e_m (u_m - v_1) + SAT|^{x_l} \qquad u \in [x_l, x_I] \tag{48}$$
$$C_2 v_t = (A \otimes D_1)v + \sigma_r A^- \otimes H^{-1} e_1 (v_1 - u_m) + SAT|^{x_r} \qquad v \in [x_I, x_r] \tag{49}$$

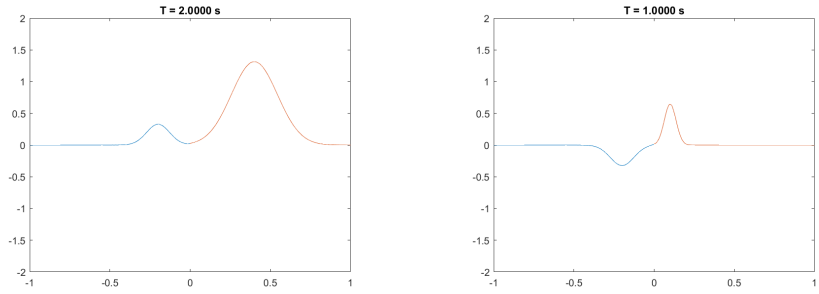

(a) solution at t=2s with $\epsilon^{(l,r)} = 4, 1$ (b) solution at t=1s with $\epsilon^{(l,r)} = 1, 4$

Figure 4: Gaussian waves after splitting at interface at x=0 using SBP-SAT with h=100

with SAT$|^{x_r}$ and SAT$|^{x_l}$ being for example the same as the boundary conditions from the SBP-SAT projection in assignment 1, and $\sigma_{l,r}$ being parameters to adjust for stability, which can be done by computing the energy estimate of the SBP-SAT approximation. $A^{+,-}$ are obtained Steger-Warming flux splitting.

$$\frac{\mathrm{d}}{\mathrm{dt}}(\|u\|^2_{HC_1} + \|v\|^2_{HC_2}) = u_m^*(A^+ + A^-)u_m + 2\sigma_l u_m^* A^+ u_m - \sigma_l u_m^* A^+ v_1 - \sigma_l v_1^* A^+ u_m + v_1^*(A^+ + A^-)v_1 + 2\sigma_r v_1^* A^+ v_1 - \sigma_r v_1^* A^+ u_m - \sigma_r u_m^* A^+ v_1 \quad (50)$$

Where A $= A^+ + A^-$ has been used. Summing up the terms we have

$$\begin{pmatrix} u_m \\ v_1 \end{pmatrix}^T A^+ \otimes \begin{pmatrix} 2\sigma_l + 1 & -\sigma_l \\ -\sigma_l & -1 \end{pmatrix} \begin{pmatrix} u_m \\ v_1 \end{pmatrix} + \begin{pmatrix} u_m \\ v_1 \end{pmatrix}^T A^- \otimes \begin{pmatrix} 1 & -\sigma_r \\ -\sigma_r & 2\sigma_r - 1 \end{pmatrix} \begin{pmatrix} u_m \\ v_1 \end{pmatrix} + SAT|^{x_r} + SAT|^{x_l} \leq 0 \quad (51)$$

For stability we want the terms associated with A^+ to be negative and the ones associated with A^- to be positive. This is achieved by putting σ_l to -1 and σ_r to 1.

2.3 Implementation

By using the initial condition of having the electric field at T=0 be the gaussian profile $\theta^{(1)}(x, 0)$ and the magnetic field the profile $\theta^{(2)}(x, 0)$ we have a right going gaussian wave.

m	$\log_{10}(\Delta)_{SAT}$	q_{SAT}
50	-1.3761	-
100	-2.3761	3.2077
200	-3.0975	2.5106
400	-3.6696	1.9006

Table 2: Convergence rate q for difference between theoretical and numerical values

Two solutions using different $\epsilon^{(l,r)}$ are given in fig. 4. For the first wave having $\eta^{(l,r)} = (2,1)$, we have the theoretical values given by 46 as T = $\frac{4}{3}$ and R = $\frac{1}{3}$, with the numerical results being T = 1.3317 and R = 0.33219. For the second figure with $\eta^{(l,r)} = (1,2)$ we have theoretical values being T = $\frac{2}{3}$ and R = $-\frac{1}{3}$, with the numerical results being 0.66211 and -0.3321.

It can also be seen that the wave in the left sub-figure travels slower, which is due to the wave-speed being given by $c^{(l)} = \frac{c}{\eta^{(l)}}$.

Taking the absolute difference between numerical and theoretical magnitudes for the waves using different h as Δ we can obtain a convergence estimate for q using $q = \frac{\log_{10}(\Delta_{m_1}/\Delta_{m_2})}{\log_{10}(m_1/m_2)}$

Taking the difference at T=1 following a left-going wave with $\epsilon^{(l,r)} = (1,4)$ like in the left part of figure 4 gives the q convergences in table 2. The convergence rate seems to be around 3 in this scenario as well.

3 Assignment 3

3.1 Boundary Conditions

We are here looking at the two-dimensional version of Maxwell's equations, given by

$$Cu_t = Au_x + Bu_y \tag{52}$$

on a square $m \times m$ domain with

$$A = \begin{pmatrix} 0 & 0 & 0 \\ 0 & 0 & -1 \\ 0 & -1 & 0 \end{pmatrix}, \quad B = \begin{pmatrix} 0 & 1 & 0 \\ 1 & 0 & 0 \\ 0 & 0 & 0 \end{pmatrix}, \quad C = \begin{pmatrix} \epsilon & 0 & 0 \\ 0 & \mu & 0 \\ 0 & 0 & \epsilon \end{pmatrix} \tag{53}$$

We can find the necessary boundary conditions by first multiplying by u from the left and doing integration by parts through which it becomes

$$(u, u_t)_C = (u, Au_x) + (u, Bu_y) = \int_{\delta S}^{\delta N} u^* Au|_{\delta W}^{\delta E} \mathrm{d}y - (u_x, Au) + \int_{\delta W}^{\delta E} u^* Bu|_{\delta S}^{\delta N} - (u_y, By)\mathrm{d}x \quad (54)$$

and then adding the transpose giving the energy estimate

$$\frac{d}{dt} \|u\|^2 = \int_{\delta S}^{\delta N} u^* Au|_{\delta W}^{\delta E} \mathrm{d}y + \int_{\delta W}^{\delta E} u^* Bu|_{\delta S}^{\delta N} \mathrm{d}x \leq 0 \quad (55)$$

For this to be less or equal to zero we can notice that

$$u^* Au|_{\delta W}^{\delta E} = -2u^{(2)}u^{(3)}|_{\delta W}^{\delta E}, \quad u^* Au|_{\delta S}^{\delta N} = -2u^{(1)}u^{(2)}|_{\delta S}^{\delta N} \quad (56)$$

which implies that one option is to set $u^{(2)}$ or $u^{(3)}$ to zero at east and west boundary and $u^{(1)}$ or $u^{(2)}$ to zero at the north and south boundary. Since the assignment specifies the electric components should be bounded this means $u^{(3)}$ at $\delta W, \delta E$ and $u^{(1)}$ at $\delta S, \delta N$.

Another possible set of boundary conditions that can be chosen are

$$\begin{cases} u^{(2)} = u^{(3)}, & x = x|^{\delta E} \\ u^{(2)} = -u^{(3)}, & x = x|^{\delta W} \\ u^{(1)} = u^{(2)}, & y = y|^{\delta N} \\ u^{(1)} = -u^{(2)}, & y = y|^{\delta S} \end{cases} \quad (57)$$

Here damping is ensured on all boundaries as the terms for the energy estimate will all be negative.

3.2 SBP-SAT

The semi-discrete SBP-SAT approximation then becomes

$$u_t = A \otimes D_x u + B \otimes D_y u + SAT_E + SAT_W + SAT_N + SAT_S \quad (58)$$

with $D_x = D_1 \otimes I_m, D_y = I_m \otimes D_1$, and

$$SAT_E = \tau_E \otimes H^{-1} e_E (u_E^{(3)} - g_E), \quad SAT_W = \tau_W \otimes H^{-1} e_W (u_W^{(3)} - g_W)$$
$$SAT_N = \tau_N \otimes H^{-1} e_N (u_N^{(1)} - g_N), \quad SAT_S = \tau_S \otimes H^{-1} e_S (u_S^{(1)} - g_S)$$

with g_E, g_W, g_N, g_S being set to zero. We can get a semi-discrete energy estimate by first multiplying with $v^T I_k \otimes H$, with k being the number of vectors

$$v^T I_k \otimes H v_t = v^T (A \otimes (Q + \frac{1}{2}B) \otimes I_m)v + v^T (B \otimes I_m \otimes (Q + \frac{1}{2}B))v + v^T \tau_E v_E^{(3)} + v^T \tau_W v_W^{(3)} + v^T \tau_E v_N^{(1)} + v^T \tau_S v_S^{(3)} \quad (59)$$

adding the transpose eliminates the Q terms and results in

$$\begin{aligned}\frac{\mathrm{d}}{\mathrm{dt}} \|u\|^2 = u_W^{(2)} u_W^{(3)} - u_E^{(2)} u_E^{(3)} + u_S^{(1)} u_S^{(2)} - u_N^{(1)} u_N^{(2)} + \\ \{\tau_E^{(1)} u_E^{(1)} u_E^{(3)} + \tau_E^{(2)} u_E^{(2)} u_E^{(3)} + \tau_E^{(3)} u_E^{(3)} u_E^{(3)}\} + \\ \{\tau_W^{(1)} u_W^{(1)} u_W^{(3)} + \tau_W^{(2)} u_W^{(2)} u_W^{(3)} + \tau_W^{(3)} u_W^{(3)} u_W^{(3)}\} + \\ \{\tau_N^{(1)} u_N^{(1)} u_N^{(1)} + \tau_N^{(2)} u_N^{(1)} u_N^{(2)} + \tau_N^{(3)} u_N^{(1)} u_N^{(3)}\} + \\ \{\tau_S^{(1)} u_S^{(1)} u_S^{(1)} + \tau_S^{(2)} u_S^{(1)} u_S^{(2)} + \tau_S^{(3)} u_S^{(1)} u_S^{(3)}\} \\ = (\tau_W^{(2)} + 1) u_W^{(2)} u_W^{(3)} + (\tau_E^{(2)} - 1) u_E^{(2)} u_E^{(3)} + (\tau_N^{(2)} + 1) u_N^{(1)} u_N^{(2)} + (\tau_S^{(2)} - 1) u_S^{(1)} u_S^{(2)} \\ + \tau_W^{(3)} u_W^{(3)} u_W^{(3)} + \tau_E^{(3)} u_W^{(3)} u_W^{(3)} + \tau_N^{(1)} u_N^{(1)} u_N^{(1)} + + \tau_S^{(1)} u_S^{(1)} u_S^{(1)} \\ + \tau_W^{(1)} u_W^{(1)} u_W^{(3)} + \tau_E^{(1)} u_E^{(1)} u_E^{(3)} + \tau_W^{(3)} u_N^{(1)} u_N^{(3)} + \tau_S^{(3)} u_S^{(1)} u_S^{(3)} \leq 0 \quad (60)\end{aligned}$$

For this to hold we need to set our parameters to

$$\tau_W = \begin{pmatrix} 0 \\ -1 \\ \leq 0 \end{pmatrix}, \quad \tau_E = \begin{pmatrix} 0 \\ 1 \\ \leq 0 \end{pmatrix}, \quad \tau_N = \begin{pmatrix} \leq 0 \\ -1 \\ 0 \end{pmatrix}, \quad \tau_S = \begin{pmatrix} \leq 0 \\ -1 \\ 0 \end{pmatrix} \quad (61)$$

with one of the values in each τ being able to be tuned to at or below zero, with 0 giving energy conservation and below 0 giving damping.

3.3 Implementation

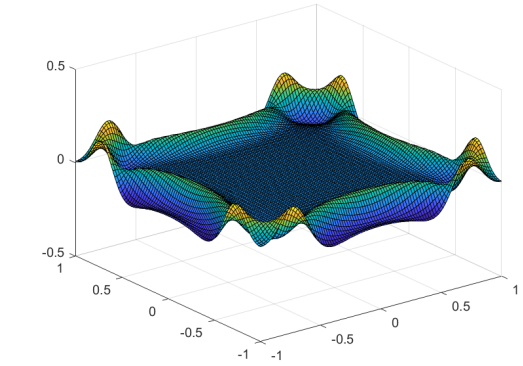

Figure 5: Solution for $H^{(z)}$ at t=1.2s

Here we implement the algorithm and measure the divergence in the electrical fields. The initial condition is given by

$$H^{(z)} = \exp(-(\frac{x - x_0}{r_*})^2 - (\frac{y - y_0}{r_*})^2) \tag{62}$$

with $x_0 = y_0 = 0$ and $r_* = 0.1$.

The divergence $\bar{\Theta}_m$ can be found using

$$\bar{\Theta}_m = D_1 \otimes I_m U + I_m \otimes D_1 V \tag{63}$$

where U and V are the numerical approximations of the $E^{(x)}$ and $E^{(y)}$ vectors.

The l_2 norm of the divergence is given by

$$\left\|\bar{\Theta}_m\right\|_{\bar{H}} = \sqrt{\bar{\Theta}_m^T (H \otimes I_m) \cdot (I_m \otimes H) \bar{\Theta}_m} \tag{64}$$

and the convergence q between two computations using grids $m \times m$ and $n \times n$ can be found using

$$q = \frac{\log\left(\frac{\left\|\bar{\Theta}_m\right\|_{\bar{H}}}{\left\|\bar{\Theta}_n\right\|_{\bar{H}}}\right)}{\log(\frac{m}{n})} \tag{65}$$

This has been computed in table 3. When using non-damping terms in the τ parameters we get a divergence near machine precision at around 5e-15 which

Non-damping			Damping		
m	$\log\|\|\bar{\Theta}_m\|\|_{\bar{H}}$	q	m	$\log\|\|\bar{\Theta}_m\|\|_{\bar{H}}$	q
50	-14.2101	-	50	-1.5544	-
100	-13.7130	-1.6515	100	-2.1249	1.8953
200	-3.0180	-35.5279	200	-2.9208	2.6439

Table 3: Convergence rate q when using non-damping and damping terms in SBP-SAT

doesn't give any conclusions for the convergence. When using damping terms we instead seem to achieve a convergence in the area of q being between 2 and 3.

3.4 Interface Conditions

We now are to calculate the Maxwell equations propagating in four domains following equations

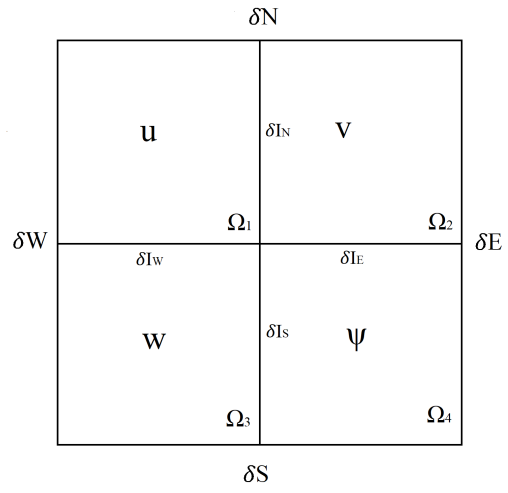

Figure 6: Computational domain in 2D with different media

$$
\begin{aligned}
C_1 u_t &= A u_x + B u_y \qquad u \in \Omega_1 \\
C_2 v_t &= A v_x + B v_y \qquad v \in \Omega_2 \\
C_3 w_t &= A w_x + B w_y \qquad w \in \Omega_3 \\
C_4 \psi_t &= A \psi_x + B \psi_y \qquad \psi \in \Omega_4
\end{aligned}
$$

With the domains Ω being given in the figure. For the boundary conditions we can apply the same as derived in the last section. For interface conditions we need to set it so that $u_E = v_W|^{\delta I_N}, w_E = \psi_W|^{\delta I_S}, u_S = w_N|^{\delta I_W}, v_S = \psi_N|^{\delta I_E}$ for all equations to be continuous.

We can see that the eigenvalues for both A and B are $\begin{pmatrix} -1 \\ 0 \\ 1 \end{pmatrix}$, which means one going towards each boundary. The positive eigenvalues will then travel from west to east and south to north, with the opposite for the negative eigenvalues. We can use the same boundary terms as in the previous part. For the interface terms, splitting the matrices into positive and negative parts using Steger-Warming flux splitting we then bound the equations by setting the A^+, B^+ matrices to negative and A^-, B^- to positive, giving:

$$\begin{aligned}
C_1 u_t = (A \otimes D_1 \otimes I_m)u + B \otimes I_m \otimes D_1)u - A^+ \otimes H^{-1} e_m \otimes I_m(u_E - v_W) + \\
B^- \otimes I_m H^{-1} e_1(u_S - w_N) + SAT_W + SAT_N \\
C_2 v_t = (A \otimes D_1 \otimes I_m)w + B \otimes I_m \otimes D_1)v + A^- \otimes H^{-1} e_1 \otimes I_m(v_W - u_E) + \\
B^- \otimes I_m H^{-1} e_1(v_S - \psi_N) + SAT_E + SAT_N \\
C_3 w_t = (A \otimes D_1 \otimes I_m)w + B \otimes I_m \otimes D_1)w - A^+ \otimes H^{-1} e_m \otimes I_m(w_E - \psi_E) - \\
B^+ \otimes I_m H^{-1} e_m(w_N - u_S) + SAT_W + SAT_S \\
C_3 \psi_t = (A \otimes D_1 \otimes I_m)\psi + B \otimes I_m \otimes D_1)\psi + A^- \otimes H^{-1} e_1 \otimes I_m(\psi_W - w_E) - \\
B^+ \otimes I_m H^{-1} e_m(\psi_N - v_S) + SAT_E + SAT_S
\end{aligned}$$

with $u_S = I_k \otimes I_m \otimes e_1^T$, $u_E = I_k \otimes e_m^T \otimes I_m$ and so on for the different vectors.

The initial conditions are implemented using $H^{(z)} = \exp(-(\frac{x-x_0}{r_*})^2 - (\frac{y-y_0}{r_*})^2)$ with $x_0 = -0.5, y_0 = 0.5, r_* = 0.1$. The ϵ for the different domains are $\epsilon = 1$ in Ω_1, Ω_2 and Ω_3 and 5 in Ω_4 from figure 6.

An example of how the solution reacts at 2 seconds is given in figure 7 with a mesh of h=201. The convergence rate q is calculated using damping and non-damping boundary terms. This time we can measure the divergence in both cases, maybe because the more complicated interface behavior leads to more divergence. The convergence rate is somewhat lower, seeming to be around 2 for both damping and non-damping.

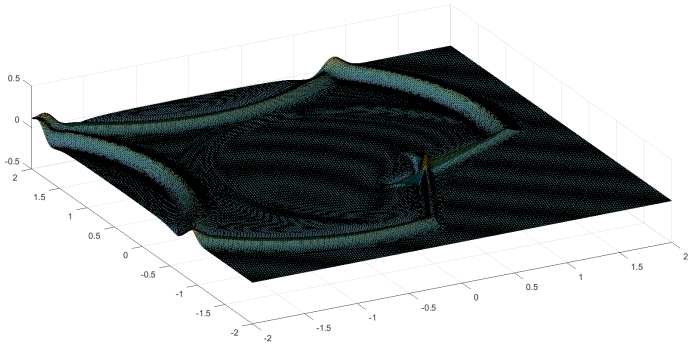

Figure 7: Solution with interface conditions at T=2s using a mesh of h=201

Non-damping			Damping		
m	$\log\|\|\Theta_m\|\|_{\bar{H}}$	q	m	$\log\|\|\Theta_m\|\|_{\bar{H}}$	q
51	-1.7696	-	51	-1.4089	-
101	-2.2518	1.6251	101	-2.1024	2.3368
201	-3.0417	2.6428	201	-2.6110	1.9961

Table 4: Convergence rate q when using non-damping and damping boundary terms in SBP-SAT